31st Congress of the International Council of the Aeronautical Sciences

Belo Horizonte, Brazil; September 09-14, 2018

ANALYSIS AND OPTIMIZATION OF ANTI-WIND CAPABILITY OF AN ELECTRIC HYBRID AERIAL VEHICLE

Hang Zhang, Bifeng Song, Hang Ma, Wen Fang
School of Aeronautics, Northwestern Polytechnical University

Keywords: *QF-HAV, anti-wind capability, analysis, optimization*

Abstract

The application of the electric quadrotor fixed-wing vertical take-off and landing (VTOL) hybrid unmanned aerial vehicle (QF-HAV) is severely limited by the poor anti-wind capability during VTOL process. This paper proposes a method that can analyze the anti-wind capability of the QF-HAV. The force equilibrium equations of the QF-HAV that hovers in the wind interference situation is established based on the simplifying of the complexity and uncertainty of the wind field by assuming that the wind is steady flow and decomposing the wind direction into two parts. The anti-wind capability of a QF-HAV with twin-boom is analyzed using the method proposed and the analysis results show that the anti-wind capability of the QF-HAV is strong in the head-wind situation and poor in the crosswind situation. Wind-induced yaw moment is the main factor that causes the QF-HAV which hovers in the wind interference situation to become unstable during VTOL process. The angle and the installation position of the propeller disc of the quadrotor are the factors that have great effects on the anti-wind capability of the QF-HAV. The anti-wind capability can be improved by optimizing the aerodynamic configuration of the QF-HAV, increasing the angle of the propeller disc and extending the distance between the installation position of the propeller disc and the center of the gravity.

1 Introduction

In recent years, Unmanned Air Vehicles (UAVs) have been widely used in both military and civilian fields due to their flexibility in configuration, low manufacturing and operating cost and not risking pilot in demanding missions, such as surveillance, tracking, environment observation, fish finding and law enforcement[1, 2]. Most of the UAV applications require UAVs that are capable of doing a wide range of different and complementary operations within a composite mission. However, conventional fixed-wing UAVs generally have good cruise performance, they can fly with high speed, long range and are within a wide range independent from wind situations, but they require a suitable air strip or special launch and recovery equipment such as catapult launchers, parachutes or nets. The helicopters and multicopters can take-off and land vertically and the flight controllers of the vehicles are mature. But the endurance and operation speed of the rotary-wing UAVs are restricted. Consequently, lots of studies have focused on fixed-wing vertical take-off and landing (VTOL) concepts that combine the advantages of fixed-wing UAVs and rotary-wing UAVs[3, 4].

There is a large number of VTOL UAV concepts such as tail-sitter, tilt-wing, tilt-rotor and compound helicopter have been studied and tested[5]. These types of platforms suffer from low efficiency, complex aerodynamic characteristics and mechanism, difficult transition manoeuvres that operate the aircraft out of trim situations and susceptibility to disturbances in transitions [6-8]. In this case, large-scale applications of these VTOL UAVs are not possible until the technological breakthrough.

Electric quadrotor fixed-wing VTOL hybrid unmanned aerial vehicle (QF-HAV), featured separating lift and thrust model is selected to simplify the control and mechanism, which is absent in tilting rotor, allows smooth transition and has advantages in control, manufacturing and

maintenance cost. This concept of VTOL UAV has the potential to be developed and widely used and is getting more and more attention. The control mode, power system and aerodynamic performance of the QF-HAV have been studied a lot[9-12]. However, the QF-HAV suffers from poor anti-wind capability during VTOL process, which limits its large-scale application severely. Thus the researches on the anti-wind capability of the QF-HAV are essential and urgent.

This paper presents a method to analyze the anti-wind capability of the QF-HAV during VTOL process. The performance of aerodynamic and the quadrotor system of a QF-HAV with twin-boom are presented and modeled to analyze the anti-wind capability. The factors that have important effects on the anti-wind capability of the QF-HAV are analyzed and the improvement and optimization measures are put forward.

2 Analysis Method

Currently, the majority of QF-HAV products and open source autopilots support two high-level control modes, namely Fully-Autonomous Control (FAC) and Semi-Autonomous Control (SAC). In the practical scenario, the FAC is most commonly used, which automatically attempts to maintain the current location, heading and attitude during VTOL process. In this case, the anti-wind capability during VTOL process is consistent with the capability of the quadrotor power system to maintain the current location, heading and attitude of the QF-HAV in the wind interference situation. Therefore, the anti-wind capability of QF-HAV can be defined as the maximum wind velocity at which the quadrotor power system can stabilize the attitude, maintain the current heading and keep the QF-HAV in place during VTOL process. The higher the maximum wind velocity, the stronger the anti-wind capability.

The wind field during VTOL process can be regarded as steady flow because of the short time. To ensure an safe taking-off and landing at high wind speed conditions, the operators usually forecast the wind speed and direction in mission planning and path planning to make sure that the QF-HAV faces the wind during VTOL process. This operation ensures that the angle between the opposite of the wind direction and the heading of the QF-HAV is between -90° and 90°. Thus the wind direction can be decomposed into two parts due to the symmetry of the QF-HAV, one is opposite to the heading of the QF-HAV and the other is perpendicular to the plane of symmetry of the QF-HAV, which can be called ‘head-wind’ and ‘crosswind’, respectively. In this paper, the anti-wind capability of the QF-HAV is analyzed independently in the head-wind situation and crosswind situation.

2.1 Coordinate Frame and Quadrotor System

A typical QF-HAV is constructed of quadrotor system and fixed-wing system. Fig. 1 illustrates the decomposition of the thrust and torque and the installation method of quadrotor system. The coordinate frames are used in this paper and the Euler angles of the QF-HAV which hovers in the wind interference situation during VTOL process is presented in Fig. 2.

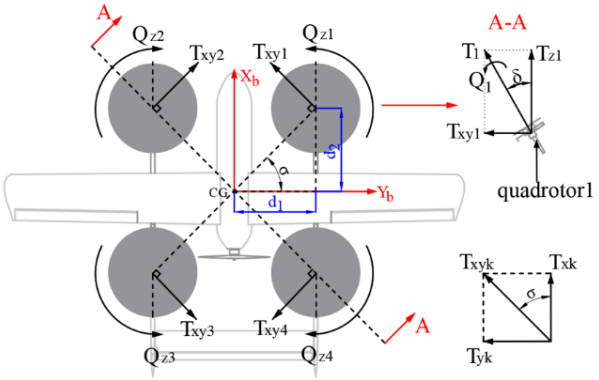

Fig. 1 Decomposition of the Thrust and Torque and the Installation Method of Quadrotor System

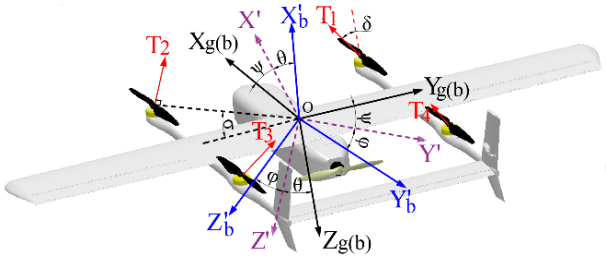

Fig. 2 The Coordinate Frames and the Euler Angles

The symbols and coordinate frames in the figures above are defined as follows:

- The body coordinate frame $OX_bY_bZ_b$ is parallel to the earth coordinate frame $OX_gY_gZ_g$ before taking-off and landing

and it coincides with $OX'_bY'_bZ'_b$ when the QF-HAV hovers in the wind interference situation during VTOL process.

- θ, φ and ψ is pitch angle, roll angle and yaw angle, respectively. α is the equivalent angle of attack and β is the equivalent sideslip angle.
- T_k and Q_k, k=1, 2, 3, 4 are the thrusts and torques of the quadrotor motor systems numbered 1-4, respectively.
- T_{xk}, T_{yk}, T_{zk} are the components of T_k and Q_{xk}, Q_{yk}, Q_{zk} are the components of Q_k on the OX_b, OY_b and OZ_b axis, respectively.
- T_{xyk}, T_{yzk}, and T_{xzk} are the components of T_k on the OX_bY_b, OY_bZ_b and OX_bZ_b coordinate planes, respectively.
- δ is the angle of propeller disc of the quadrotor.
- σ is the angle between the line of diagonally opposite quadrotor motors and Y_b axis.
- d_1 and d_2 are the distance between the installation position of propeller disc of the quadrotor and the Y_b and X_b axis, respectively.
- v is the wind velocity.

2.2 Head-Wind Situation

The QF-HAV that hovers in the head-wind situation can keep sabilization by nose down due to the airframe symmetry. Figure 3 illustrates the force analysis of the QF-HAV in this situation.

The gravity and aerodynamic forces are projected onto the body coordinate frame by the following equations for convenience[13]:

$$\begin{bmatrix} G_x & G_y & G_z \end{bmatrix}^T = P_g^b \begin{bmatrix} 0 & 0 & mg \end{bmatrix}^T \quad (1)$$

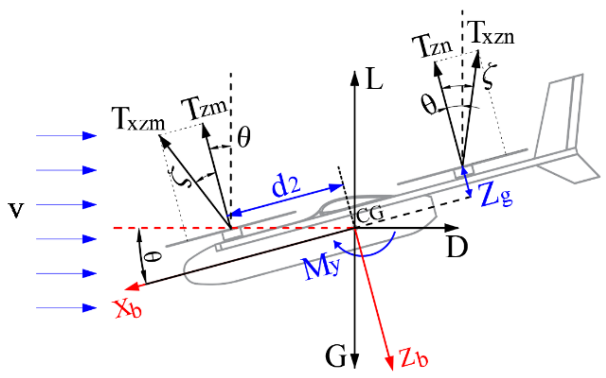

Fig. 3 The Force Analysis In the Head-Wind Situation

$$\begin{bmatrix} F_x & F_y & F_z \end{bmatrix}^T = P_w^b \begin{bmatrix} -D & Y & -L \end{bmatrix}^T \quad (2)$$

where P_g^b is the transformation matrix from the earth coordinate frame to the body coordinate frame. P_w^b is the transformation matrix from the wind coordinate frame to the body coordinate frame. In this situation, the equations $\theta = \alpha$ and $\psi = \varphi = \beta$ are established and substituted into the transformation matrixes to yield

$$P_w^b = P_g^b = \begin{bmatrix} \cos\theta & 0 & -\sin\theta \\ 0 & 1 & 0 \\ \sin\theta & 0 & \cos\theta \end{bmatrix} \quad (3)$$

Then the following equations can be established if the QF-HAV has anti-wind capability:

$$-\sum_{k=1}^{4} T_{zk} + G_z + F_z = 0 \quad (4)$$

$$\sum_{m=1,2} T_{xm} - \sum_{n=3,4} T_{xn} + G_x + F_x = 0 \quad (5)$$

$$\left(\sum_{m=1,2} T_{zm} - \sum_{n=3,4} T_{zn}\right) d_2 + \left(\sum_{n=3,4} T_{xn} - \sum_{m=1,2} T_{xm}\right) Z_g + \left(\sum_{i=2,3} Q_{yi} - \sum_{j=1,4} Q_{yj}\right) + M_y = 0 \quad (6)$$

Where L, D and M_y are lift, drag and pitch moment of the QF-HAV. Z_g is the vertical distance from the center of propeller disc of the quadrotor to the position of the center of gravity. The forces and moments meet the following equations:

$$L = 1/2\rho v^2 C_L S \quad (7)$$

$$D = 1/2\rho v^2 C_D S \quad (8)$$

$$M_y = 1/2\rho v^2 C_m S c \quad (9)$$

$$T_1 = T_2, T_3 = T_4 \quad (10)$$

$$T_{xk} = T_k \sin\delta\cos\sigma \quad (11)$$

$$T_{zk} = T_k \cos\delta \quad (12)$$

$$T_k \le T_{k\max}, \quad T_{k\max} \propto \frac{1}{V_{Tk}} \quad (13)$$

$$Q_{yk} = Q_k \sin\delta\sin\sigma, \quad Q_k \propto T_k \quad (14)$$

where V_{Tk} is the axial flow velocity of the quadrotor propellers. ζ is the angle between T_{xzk} and T_{zk} and it is usually small. Thus V_{Tk} can be approximately obtained as follows

$$V_{T1} = V_{T2} = v\sin(\zeta + \theta) \quad (15)$$

$$V_{T3} = V_{T4} = v\sin(|\zeta - \theta|) \quad (16)$$

2.3 Crosswind Situation

The changes of the attitude of the QF-HAV that hovers in the crosswind situation are much more complex. In this situation, the force analysis of the QF-HAV is shown in figure 4. The relations between the equivalent angle of attack, equivalent sideslip angle and the Euler angles can be discribed as follows:

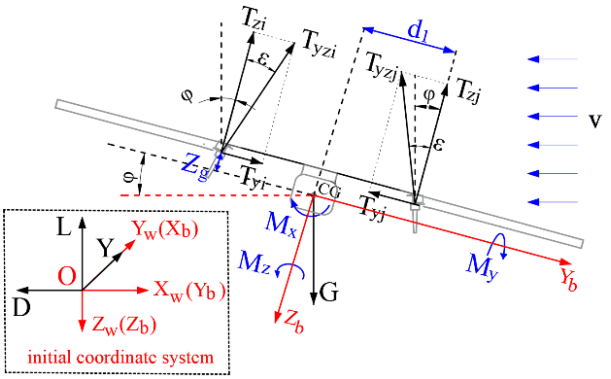

Fig. 4 The Force Analysis In the Crosswind Situation

$$\alpha=\theta \tag{17}$$

$$\beta=-90°+\psi \tag{18}$$

The aerodynamic forces and the gravity can be projected onto the body coordinate frame using the Eqs. (1) and (2). Then the following relation between P_g^b and P_w^b exists:

$$P_w^b=P_g^b(\psi=-\beta,\theta=\alpha) \tag{19}$$

P_g^b is described by the Eq. (20). The QF-HAV has anti-wind capability means that it is in static equilibrium when it hovers in the crosswind situation. This equilibrium state can be described by Eq. (21).

$$P_g^b=\begin{bmatrix} \cos\theta\cos\psi & \cos\theta\sin\psi & -\sin\theta \\ \sin\theta\sin\varphi\cos\psi-\sin\psi\cos\varphi & \sin\psi\sin\theta\sin\varphi+\cos\psi\cos\varphi & \sin\varphi\cos\theta \\ \sin\theta\cos\varphi\cos\psi+\sin\psi\sin\varphi & \sin\psi\sin\theta\cos\varphi-\cos\psi\sin\varphi & \cos\varphi\cos\theta \end{bmatrix} \tag{20}$$

$$\begin{bmatrix} \sum_{m=1,2}T_{xm}-\sum_{n=3,4}T_{xn} & 0 & G_x & F_x \\ \sum_{i=2,3}T_{yi}-\sum_{j=1,4}T_{yj} & 0 & G_y & F_y \\ \sum_{k=1}^{4}T_{zk} & 0 & G_z & F_z \\ \sum_{i=2,3}T_{zi}-\sum_{j=1,4}T_{zj} & \sum_{i=2,3}T_{yi}-\sum_{j=1,4}T_{yj} & \sum_{j=1,4}Q_{xj}-\sum_{i=2,3}Q_{xi} & M_x \\ \sum_{m=1,2}T_{zm}-\sum_{n=3,4}T_{zn} & \sum_{n=3,4}T_{xn}-\sum_{m=1,2}T_{xm} & \sum_{n=3,4}Q_{yn}-\sum_{m=1,2}Q_{ym} & M_y \\ \sum_{p=2,4}T_{yp}-\sum_{q=1,3}T_{yq} & \sum_{p=2,4}T_{xp}-\sum_{q=1,3}T_{xq} & \sum_{p=2,4}Q_{zp}-\sum_{q=1,3}Q_{zq} & M_z \end{bmatrix} \begin{bmatrix} 1 & 1 & -1 & d_1 & d_2 & d_2 \\ 0 & 0 & 0 & Z_g & Z_g & d_1 \\ 1 & 1 & 1 & 1 & 1 & 1 \\ 1 & 1 & 1 & 1 & 1 & 1 \end{bmatrix}=0 \tag{21}$$

where the thrusts, moments and their components are calculated as follows:

$$F_{xk}=T_k\sin\delta\cos\sigma \tag{22}$$

$$F_{yk}=T_k\sin\delta\sin\sigma \tag{23}$$

$$F_{zk}=T_k\cos\delta \tag{24}$$

$$Q_{xk}=Q_k\sin\delta\cos\sigma \tag{25}$$

$$Q_{yk}=Q_k\sin\delta\sin\sigma \tag{26}$$

$$Q_{zk}=Q_k\cos\delta \tag{27}$$

$$T_k\le T_{k\max},\quad T_{k\max}\propto\frac{1}{V_{Tk}} \tag{28}$$

$$Q_k\propto T_k \tag{29}$$

ε is defined as the angle between T_{yzk} and T_{zk} and it is satisfied

$$\tan\varepsilon=\sin\sigma\tan\delta \tag{30}$$

The axial flow velocity of the quadrotor propellers can be approximately given by the following equations:

$$V_{T2}=V_{T3}=v\sin(\varphi+\varepsilon) \tag{31}$$

$$V_{T1}=V_{T4}=v\sin(|\varphi-\varepsilon|) \tag{32}$$

3 Analysis of the Anti-Wind Capability of a QF-HAV

The anti-wind capability of a QF-HAV with twin-boom is analyzed to vertify the correctness of the mothod proposed in this section. The configuration of the QF-HAV is presented in Fig. 5 and the conceptual and configuration parameters are given in Table 1.

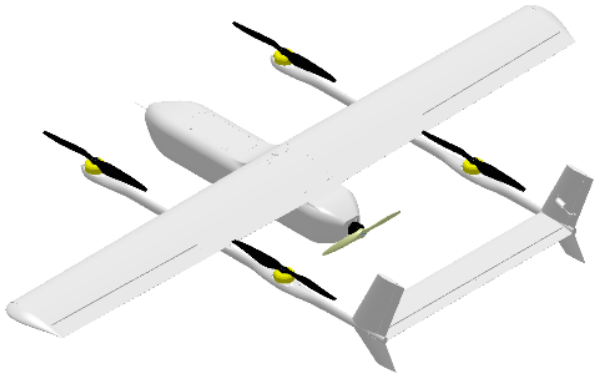

Fig. 5 The Configuration of the QF-HAV

Table 1 Conceptual and Configuration Parameters

Parameter	Value
Aspect Ratio(AR)	9
Wing area(S)	1.6m^2
$(T/W)_{VTOL}$	2
$(T/W)_{FW}$	0.4
Maximum takeoff weight(G)	30kg
δ	0°
σ	45°
d_1	0.7m
d_2	0.7m
Z_g	0.18m

3.1 Performance of the QF-HAV

3.1.1 Aerodynamic Performance

The aerodynamic coefficients are calculated using CFD method in the situations of the wind speed of 11m/s and the altitude of 1km. The computational parameters are shown in Table 2.

Table 2 Computational Parameters

Direction	$\theta(\alpha)$ /deg	φ /deg	ψ /deg	Interval
Head-wind	-20~20	0	0	2°
Crosswind	-10~10	-20~20	-15~15	5°

The computing results in the head-wind situation which conclude the lift coefficient, drag coefficient and pitch moment coefficient are shown in Fig. 6. The computing results that conclude the lift coefficient, drag coefficient, side force coefficient, pitch moment, roll moment and yaw moment in the crosswind situation are hard to illustrate because of the four dimensional characteristics. In this situation, the Kriging approximation model is used to fit the relations between the aerodynamic coefficients and the Euler angles for the convenience of calling data during the analysis process.

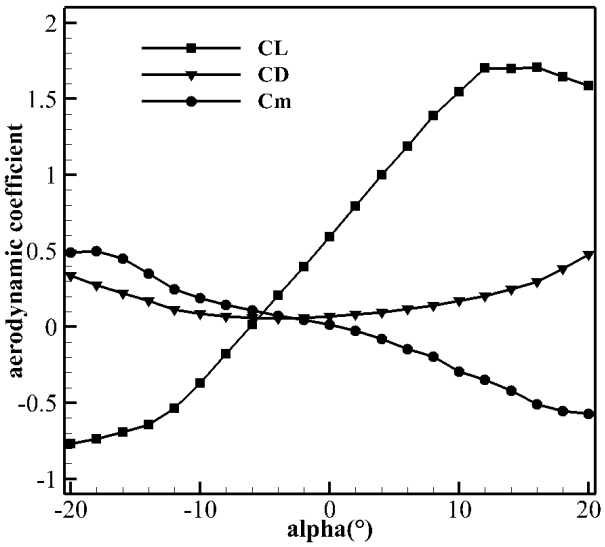

Fig. 6 The Aerodynamic Coefficients (Head-wind)

3.1.2 Quadrotor Power System Performance

The axial flow speed of the quadrotor propellers is usually low and the effect of the axial flow on the relation between the thrust and the torque of the quadrotor power system can be negligible.

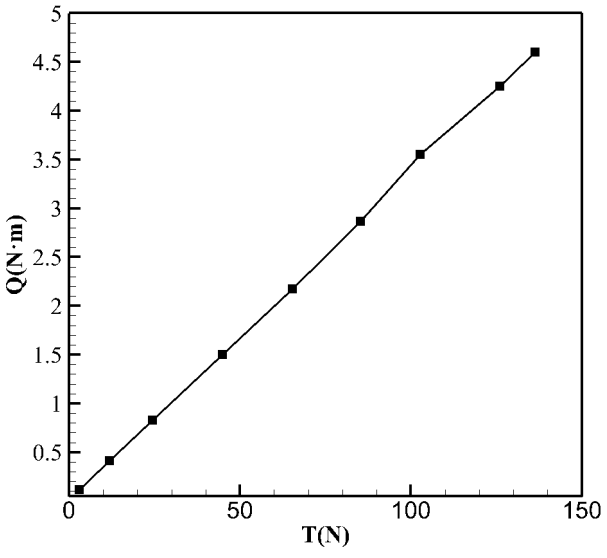

Fig. 7 The Relation Between T_k and Q_k

Thus the relation between the thrust and the torque of the quadrotor power system during VTOL process can be approximated by the relation between the static thrust and the torque. The relation is illustrated in Fig. 7.

The test result shows that the maximum quadrotor motor speed is about 4000 r/min. In this case, as is presented in Fig. 8, the relation between the maximum thrust and the axial flow speed of the quadrotor propellers is calculated using QPROP program.

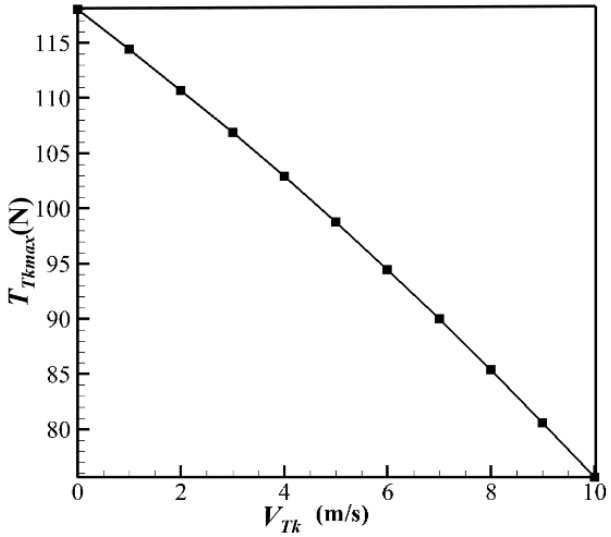

Fig. 8 The Relation Between T_{kmax} and V_{Tk}

3.2 Anti-Wind Capability Analysis

3.2.1 Head-Wind Situation

As shown in Fig. 9, substituting the aerodynamic coefficients and the relations between the performance parameters of the quadrotor power system into Eqs. (1) to (16) yields the relation between the pitch angle and the wind velocity at which the QF-HAV in hover could keep stabilization. The relations between the thrust (T_k) of each quadrotor motor system, the aggregate thrust (T_{tot}) of the quadrotor power system and the wind velocity are presented in Fig.10.

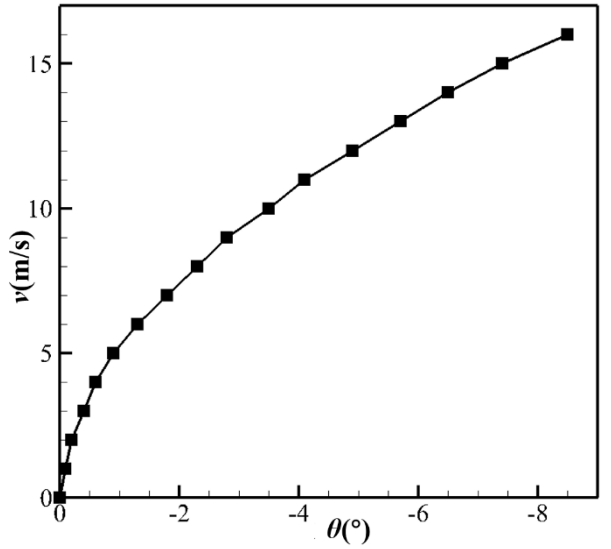

Fig. 9 The Relation Between v and θ

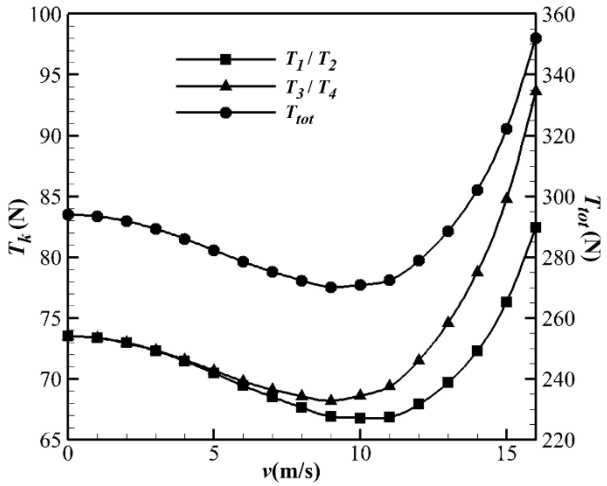

Fig. 10 The Relations Between T_k, T_{tot} and v

The relation in Fig. 9 indicates that the maximum wind velocity at which the QF-HAV in hover could keep stabilization is 15m/s in the head-wind situation, which means that the QF-HAV has strong anti-wind capability and can adapt to the most of the application environment.

An important result can be seen from Fig.10 that T_k and T_{tot} decrease first and then increase with the increase of the wind speed. The reason for the decrease of the thrust with the increase of the wind speed in the range 0 to 9m/s is that the pitch angle is greater than the zero-lift angle when the QF-HAV hovers in the wind interference situation because of the positive incidence angle and the negative zero-lift angle of the wing. When the wind speed increases in this range, the decrease of the lift coefficient with the decrease of the pitch angle is smaller than the increase of the square of the wind velocity. In this case, the lift produced by the wing increases according to Eq. (7) which reduces the required thrust of the quadrotor power system. The lift coefficient decreases sharply with the decrease of the pitch angle which reduces the lift produced by the wing when the wind speed is greater than 9m/s. The lift is further reduced to negative when the pitch angle is less than the zero-lift angle. For

this reason, the required thrust of the quadrotor power system increases gradually with the increase of the wind speed and the increase rate of the required thrust increases. This result indicates that suitable wind speed can be used to reduce the power consumption of the quadrotor power system in practice.

It is evident from Fig. 10 that the thrusts numbered T_1 and T_2 are less than the thrusts numbered T_3 and T_4. This is because the difference of the thrusts of the quadrotor motor systems can balance the aerodynamic drag and the pitch moment to keep the QF-HAV stabilization.

3.2.2 Crosswind Situation

Substituting the Kriging approximation model established above and the relations between the performance parameters of the quadrotor power system into Eqs. (17) to (32) obtains the relation between the Euler angles and the wind velocity at which the QF-HAV in hover could keep stabilization. The lower boundary of the result is illustrated in Fig. 11.

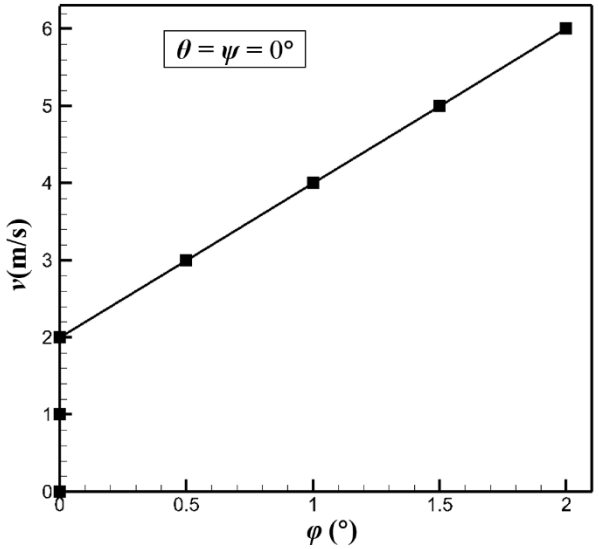

Fig. 11 The Relation Between *v* and the Euler Angles

We can see from Fig.11 that the maximum wind speed at which the QF-HAV in hover could keep stabilization is 6m/s. The reason why the attitude of the QF-HAV has not changed when the wind speed is less than 2m/s is the Euler angles are too small to be recorded and illustrated. It is apparent that the anti-wind capability of the QF-HAV is poor in this situation, which limits the applications of the QF-HAV.

4 Optimization and Improvement

As indicated above, the analysis results show that the anti-wind capability of the QF-HAV is strong in the head-wind situation and poor in the crosswind situation, which are consistant with the practical situation. Therefore, this section focuses on the factors that affect the anti-wind capability of the QF-HAV in the crosswind situation.

The parameters in the Eq. (21) reveals that the factors that affect the anti-wind capability of the QF-HAV conclude the configuration parameters (d_1, d_2, Z_g and δ) and the aerodynamic parameters (L, D, Y, M_x, M_y and M_z). The main effect of the factors is analyzed using the design of experiment method. Optimal Latin hypercube design is used to generate the sample data. The number of the levels of the factors is set to 2000. The upper and lower boundaries of the range of the configuration parameter values are ±20% of the current values. The range of the aerodynamic parameter values is consistent with the range of the CFD results. The Pareto diagram about the effect of each parameter on the anti-wind capability of the QF-HAV is shown in Fig.12.

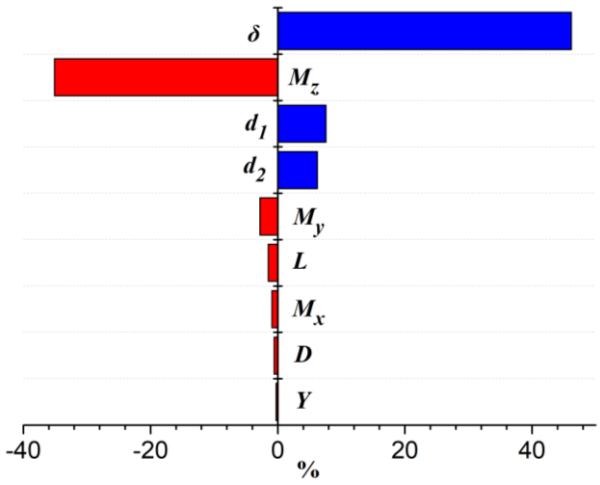

Fig. 12 The Pareto Diagram

It can be seen from the Pareto diagram that δ, M_z, d_1 and d_2 are the parameters that have great effects on the anti-wind capability of the QF-HAV and these parameters account for more than 95% of the effects. M_z has negative effect on the anti-wind capability, which means that wind-induced yaw moment is the main factor that causes the QF-HAV which hovers in the wind interference situation to become unstable during

VTOL process. The yaw control moment produced by the quadrotor power system consists of the torque reactions of the quadrotor motor systems and the yaw moment produced by the components of the thrusts of the quadrotor motor systems. The increasing of δ can increase the component of the thrust and the extending of d_1 and d_2 can increase the arm of force of the yaw control moment. Both of them can increase the yaw control moment, which account for the positive effects of δ, d_1 and d_2 on the anti-wind capability.

5 Conclusion

With the method proposed in this paper, the anti-wind capability of the QF-HAV can subsequently be analyzed and evaluated. The factors that have effects on the anti-wind capability can be intuitively obtained from the analysis model. The performance of aerodynamic and the quadrotor power system of a QF-HAV with twin-boom is presented and modeled to analyze the anti-wind capability. The analysis results show that the anti-wind capability of the QF-HAV with twin-boom is strong in the head-wind situation and poor in the crosswind situation. The angle of propeller disc of the quadrotor, the yaw moment and the distance between the installation position of the propeller disc of the quadrotor and X_b, Y_b axis are the factors that have great effects on the anti-wind capability of the QF-HAV.

The angle of propeller disc of the quadrotor has the greatest effect on the anti-wind capability and it is also the parameter that is one of the most easily changed for a QF-HAV that has been designed. Thus it is the most economical and quick method to improve the anti-wind capability by increasing the angle of propeller disc of the quadrotor. Improving the anti-wind capability by reducing the yaw moment and extending the distance between the installation position of the propeller disc of the quadrotor and X_b, Y_b axis can help design new QF-HAV with strong anti-wind capability, but it is difficult to be implemented on the QF-HAV that has been designed.

References

[1] U Ozdemir, Y O Aktas, A Vuruskan, et al. Inalhan. Design of a commercial hybrid VTOL UAV system. *Journal of Intelligent & Robotic Systems*, vol. 74, No.1-2, pp 371-393, 2014.

[2] A Idries, N Mohamed, I Jawhar, et al. Challenges of developing UAV applications: a project management view. *Proceedings of the 2015 International Conference on Industrial Engineering and Operations Management*, Dubai, pp 1-10, 2015.

[3] Z Öznalbant and M S Kavsaoglu. Design and flight test study of a VTOL UAV. *53rd AIAA Aerospace Sciences Meeting*, Kissimmee, AIAA 2015-1903, pp 1-16, 2015.

[4] K Muraoka, N Okada and D Kubo. Quad tilt wing VTOL UAV: Aerodynamic characteristics and prototype flight. *AIAA Infotech@Aerospace Conference*, Seattle, AIAA 2009-1834, pp 1-10, 2009.

[5] B Yuksek, A Vuruskan, U Ozdemir,et al. Transition flight modeling of a fixed-wing VTOL UAV. *Journal of Intelligent & Robotic SYSTES*, vol. 84, No.1-4, pp 1-23, 2016.

[6] F P Thamm, N Brieger, K P Neitzke, et al. Songbird - an innovative UAS combining the advantages of fixed wing and multi rotor UAS. *International Conference on Unmanned Aerial Vehicles in Geomatics*, Toronto, vol. XL-1/W4, pp 345-349, 2015.

[7] S Chowdhury, V Maldonado and R Patel. Conceptual design of a multi-ability reconfigurable unmanned aerial vehicle (UAV) through a synergy of 3D CAD and modular platform planning. *15th AIAA/ISSMO Multidisciplinary Analysis and Optimization Conference*, Atlanta, AIAA 2014-2178, pp 1-13, 2014.

[8] E Cetinsoy, S Dikyar, C Hancer, et al. Design and construction of a novel quad tilt-wing UAV. *Mechatronics*, vol. 22, No. 6, pp 723-745, 2012.

[9] Ç Ferit and L M Kemal. Analysis of a UAV that can hover and fly level. *2016 International Conferences on Frontiers of Sensors Technologies*, Hong Kong, Vol. 59, 07010, pp 1-5, 2016.

[10] G Anil, A K Bilge and K D Funda. Attitude and altitude stabilization of fixed wing VTOL unmanned air vehicle. *AIAA Modeling and Simulation Technologies Conference*, Washington, AIAA 2016-3378, pp1-13, 2016.

[11] D Guillaume and H Minh-Duc. Modeling of an unmanned hybrid aerial vehicle. *2014 IEEE Conference on Control Applications*, Antibes, pp 1011-1016, 2014.

[12] P T Dewi, G S Hadi, K.M Ramadhan, et al. Design of separate lift and thrust hybrid unmanned aerial vehicle. *The Journal of Instrumentation, Automation and Systems*, vol. 2, No. 2, pp. 45-51, 2015.

[13] B N Pamadi. *Performance, stability, dynamics, and control of airplanes*. Second Edition, AIAA, 2015.

6 Contact Author Email Address

Email: tjzhhang@163.com

Copyright Statement